

Biped Gait Generation based on Parametric Excitation by Knee-joint Actuation

Yuji Harata, Fumihiko Asano, Zhi-Wei Luo, Kouichi Taji and Yoji Uno

Abstract—Restoring mechanical energy lost by heel-strike collisions is necessary for stable gait generation. One principle to realize this is parametric excitation. Recently, Asano et al. applied this principle to a biped robot with telescopic-legs, and succeeded in generating a sustainable biped gait by computer simulation. In this paper, we deal with a model of a biped robot that has not only semicircular feet but also actuated knees. Though this robot has no actuator at the hip, knee actuators can sustain gait by parametric excitation. We first verify that an actuated knee can cause parametric excitation, and then show by computer simulation that the proposed biped robot can walk continuously with actuated knees only.

I. INTRODUCTION

Many biped robots have been developed. Most of them are controlled by the methods based on ZMP (Zero Moment Point) proposed by Vukobratović [9]. While ZMP based methods have succeeded to make actual biped robots walking, many researchers are interested in higher energy efficient gait generation. Passive dynamic walking [8], in which a biped robot walks continuously and stably down the slope by the gravity with no any mechanical input, has been thought as one of the most energy efficient walking approaches and has received much attentions. When we try to realize passive dynamic like walking on the level ground, we face a problem that the kinetic energy dissipates on impact of a robot's swing-leg against the ground. In other words, the restoration of mechanical energy is necessary for the sustainable gait generation. In passive dynamic walking, the kinetic energy is restored by transporting potential energy to kinetic energy in descending an incline. However, on the level ground the energy restoration by gravity can not be expected. Therefore, it is necessary to restore the kinetic energy by certain mechanical input, such as ankle torque, hip torque and so on. Asano et al. [3] proposed a so-called virtual passive dynamic walking in which the virtual gravity was designed adequately by ankle and hip torque to restore kinetic energy dissipating on impact. Goswami et al. [5] proposed energy tracking control that the ankle and hip torque were designed to make energy level constant in the sustainable gait and showed that the energy tracking control

made stable limit cycle. Asano et al. [1] also applied the virtual passive dynamic walking approach to a biped robot with semicircular feet whose support-leg rotated around the contact point between sole and ground. They have shown that the rolling of semicircular feet has similar effect of ankle torque, and hence, the robot can restore the energy dissipated on impact by only hip torque so as to generate a sustainable gait.

Another approach for restoring kinetic energy is parametric excitation which is a principle to increase amplitude of vibration by swinging itself. Asano et al. [2] applied a parametric excitation method to the biped robot with telescopic actuator in its legs. They showed that energy restoration was realized by elongating and contracting swing-leg. The telescopic-legs have another advantage that elongating and contracting swing-leg resolves the problem of digging the ground. However, their model has special mechanisms unlike human beings.

We have dealt with a kneed biped model with semicircular feet. For this robot, we applied the method based on a virtual constraint so as not to dig the ground, and generated a sustainable gait in a numerical simulation [6]. In this paper, we consider biped gait generation based on parametric excitation using a kneed biped model. It is shown that bending and stretching a knee also have the similar effect of elongating and contracting a swing-leg of the telescopic-leg, in which mechanical energy may restore by moving up and down center of mass of the swing-leg like the telescopic-legs. We first verify that the total mechanical energy of a biped robot increases by the motion of swing-leg. Then we show that a sustainable gait can be generated by this approach in numerical simulations.

This paper is organized as follows: Section II explains the biped robot with semicircular feet. Section III is a main part in this paper, in which we first explain parametric excitation and gait generation based on parametric excitation and then verify that parametric excitation approach increases total mechanical energy of a biped robot (Section III-A). We also apply parametric excitation to a biped robot with knees (Section III-B, III-C). Section IV discusses the effect of parameters. Finally, Section V gives our conclusion.

II. A MODEL OF THE PLANAR KNEED BIPED ROBOT WITH SEMICIRCULAR FEET

Fig. 1 illustrates the biped robot dealt with in this paper. The robot has four mass points and three degree of freedom, and has semicircular feet whose center is on the leg. Because there are two mass on the leg, the support-leg has inertia

Y. Harata, K. Taji and Y. Uno are with Department of Mechanical Science and Engineering, Graduate School of Engineering, Nagoya University, Furo-cho, Chikusa, Nagoya, 464-8603, Japan {y.harata, taji, uno}@nuem.nagoya-u.ac.jp

F. Asano and Z.W. Luo are with BMC RIKEN, 2271-130, Anagahora, Shimoshidami, Moriyama-ku Nagoya, 463-0003 Japan {asano, luo}@bmc.riken.jp

Z.W. Luo is with Department of Computer and Systems Engineering, Graduate School of Engineering, Kobe University, 1-1 Rokkodai, Nada, Kobe 657-8501 Japan

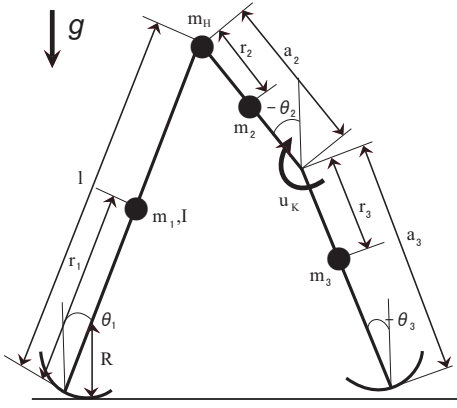


Fig. 1. Model of a planar kneed biped robot with semi-circular feet.

moment. The dynamic equation in single support phase is given by

$$\mathbf{M}(\boldsymbol{\theta})\ddot{\boldsymbol{\theta}} + \mathbf{C}(\boldsymbol{\theta}, \dot{\boldsymbol{\theta}})\dot{\boldsymbol{\theta}} + \mathbf{g}(\boldsymbol{\theta}) = \mathbf{S}u_K - \mathbf{J}^T\lambda, \quad (1)$$

where $\boldsymbol{\theta} = [\theta_1 \ \theta_2 \ \theta_3]^T$ is the generalized coordinate vector, \mathbf{M} is the inertia matrix, \mathbf{C} is the Coriolis force and the centrifugal force, and \mathbf{G} is the gravity matrix. $\mathbf{J} = \begin{bmatrix} 0 & 1 & -1 \end{bmatrix}$ and $\lambda \in \mathbb{R}$ is its binding force. The control input vector, $\mathbf{S}u_K$, is described in detail later (Section III-B). In this robot, collisions occur at the knee and the ground. Therefore the robot has three phases.

- 1st phase (Single support phase I): The support-leg rotates around the contact point between the sole and the ground, and the swing-leg is bended.
- 2nd phase (Single support phase II): The support-leg rotates around the contact point and the knee of swing-leg is locked in a straight posture. When the first phase changing to the second phase, a collision occurs at the knee.
- 3rd phase (Double support phase): This phase occurs instantaneously, and the support-leg and the swing-leg are exchanged after the collision at the ground.

When the knee straightens, a completely inelastic collision is assumed to occur at the knee of a swing-leg. The relation between before and after knee impact, $\dot{\boldsymbol{\theta}}^-$ and $\dot{\boldsymbol{\theta}}^+$ is given by

$$\mathbf{M}\dot{\boldsymbol{\theta}}^+ = \mathbf{M}\dot{\boldsymbol{\theta}}^- + \mathbf{J}^T\lambda_I, \quad (2)$$

where λ_I is constraint force which makes $\dot{\theta}_2^+ = \dot{\theta}_3^+$. This force is given by

$$\lambda_I = -\mathbf{X}_I^{-1}\mathbf{J}\dot{\boldsymbol{\theta}}^- \quad \text{and} \quad \mathbf{X}_I = \mathbf{J}\mathbf{M}^{-1}\mathbf{J}^T \quad (3)$$

From this force, angular velocities after knee impact are given by

$$\dot{\boldsymbol{\theta}}^+ = -(\mathbf{I} - \mathbf{M}^{-1}\mathbf{J}^T\mathbf{X}_I^{-1}\mathbf{J})\dot{\boldsymbol{\theta}}^-. \quad (4)$$

We also assume that, once after collision, knee-joint's is bound by the force $\mathbf{J}^T\lambda$ until completely inelastic collision at the ground.

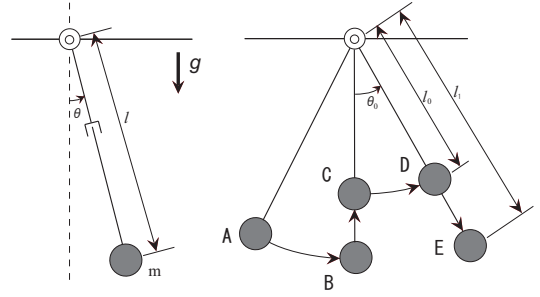


Fig. 2. Optimal trajectory of pendulum for parametric excitation.

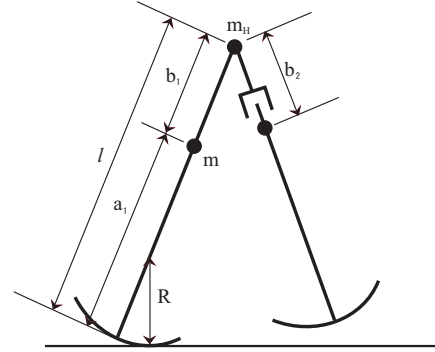


Fig. 3. Three link model of a planar underactuated biped robot with telescopic-legs.

III. PARAMETRIC EXCITATION

The parametric excitation is a phenomenon that amplitude of vibration increases by swinging itself. Fig. 2 presents the optimal trajectory, $A \rightarrow B \rightarrow C \rightarrow D \rightarrow E$, given by Lavrovskii and Formalskii [7], along which the increase of total mechanical energy is maximized, supposed that the length of a pendulum, l , is changed instantaneously. However, the length can not be actually changed instantaneously, and a reference trajectory close to the optimal trajectory is chosen to restore total mechanical energy. Asano et al. [2] applied parametric excitation principle to a biped robot with telescopic-legs by pumping the swing-leg mass. The telescopic-leg length, b_2 , in Fig. 3 is controlled to track the reference trajectory. For example, considering smooth pumping motion, they have introduced the time-dependent trajectory, $b_{2d}(t)$, as

$$b_{2d} = \begin{cases} b_1 - A_m \sin^3\left(\frac{\pi}{T_{set}}t\right) & (t \leq T_{set}) \\ b_1 & (t > T_{set}), \end{cases} \quad (5)$$

where b_1 is the distance between hip and mass point when telescopic-leg is straightened, A_m is desired amplitude of vibration, and T_{set} is the desired settling-time which is assumed before heel-strike collisions. In the other words, the condition $T \geq T_{set}$ should always hold for the steady-step period, T [s]. We call this the settling-time condition. Fig. 4 shows the simulation result of parametrically excited dynamic bipedal walking by swing-leg actuation. It can be seen that stable dynamic level locomotion is achieved without taking the ZMP condition into account since this robot does not require ankle-joint torque.

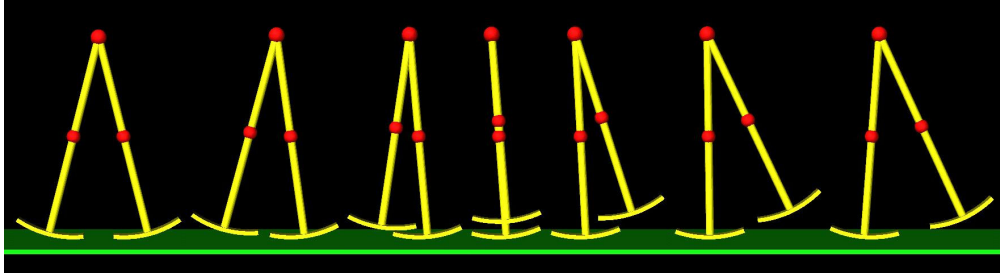


Fig. 4. Parametrically excited dynamic bipedal walking by swing-leg actuation [2].

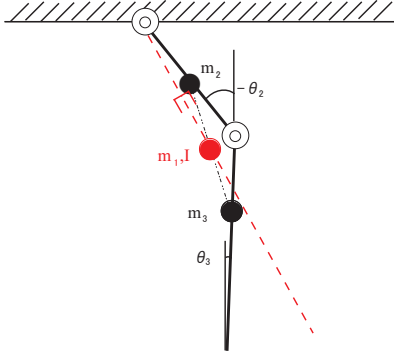


Fig. 5. Double pendulum and its equivalent 1-link model with prismatic joint.

A. Parametric excitation of a double pendulum

It was shown that total mechanical energy of a biped robot with telescopic-legs was restored by the parametric excitation approach. We verify that total mechanical energy of a biped robot with knees can also increase by the parametric excitation approach. A double pendulum, of which only the joint between two links is actuated, mimics a kneed-actuation leg. We note that the pendulum does not strike the ground, but a collision at a joint occurs like a biped robot when a joint is straightened. The dash line in Fig. 5 illustrates a virtual telescopic pendulum which connects a support point and center of mass of the pendulum. This virtual telescopic pendulum is controlled to track the reference trajectory. For simplicity, the reference trajectory is given for a relative angle by

$$(\theta_2 - \theta_3)_d = \begin{cases} A_m \sin^3\left(\frac{\pi}{T_{set}}t\right) & (t \leq T_{set}) \\ 0 & (t > T_{set}). \end{cases} \quad (6)$$

The joint is actuated during only the half cycle. Figs. 6-8 show the result of numerical simulation. The total mechanical energy is shown in Fig. 6, Fig. 7 is the enlarged illustration of Fig. 6, and Fig. 8 shows the distance between a support point and center of mass of the pendulum. Fig. 6 shows that total mechanical energy increases during the one cycle. It is observed from Figs. 7 and 8, that the total mechanical energy increases when bending and that the total energy decreases when straightening. We have assumed that the collision at a joint occurs, but mechanical energy is not dissipated in Fig. 7. This is because the relative angular velocities, $\dot{\theta}_2 -$

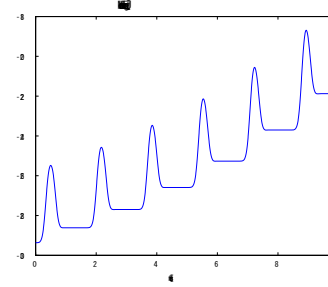


Fig. 6. Total mechanical energy of a double pendulum.

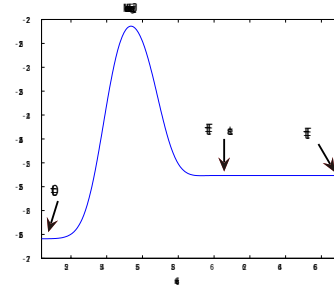


Fig. 7. Enlarged illustration of Fig. 6.

$\dot{\theta}_3$, is very close to zero at the collision. From this result it is expected that a sustainable gait of biped robots with knees can be generated by the approach based on parametric excitation principle.

B. Gait generation on a rotary actuation system based on parametric excitation principle

The distance between the hip and the center of mass of a swing-leg is given by

$$L_c = \frac{1}{m_2 + m_3} \sqrt{F_1 + F_2 \cos(\theta_2 - \theta_3)}, \quad (7)$$

where

$$F_1 = m_2^2 r_2^2 + m_3^2 (a_2^2 + r_3^2) + 2m_2 m_3 r_2 a_2 \quad (8)$$

and

$$F_2 = 2m_3^2 a_2 r_3 + 2m_2 m_3 r_2 r_3. \quad (9)$$

In the kneed biped robot with semicircular feet, collisions occur at the knee and the ground. Then, it is important to reduce energy dissipation on collisions and restore total energy

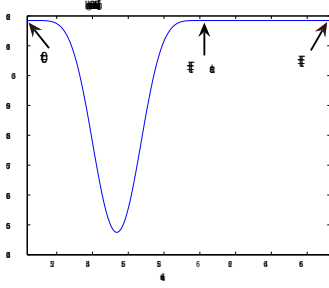


Fig. 8. Distance between a support point and center of mass of the pendulum.

as much as possible. The optimal trajectory of parametric excitation principle is shown by Fig. 2. In this paper we give heuristically the reference trajectory as

$$L_{cd} = \begin{cases} a - A_m \sin^{11}\left(\frac{\pi}{T_{set}}t\right) & (t \leq T_{set}), \\ a & (t > T_{set}), \end{cases} \quad (10)$$

where $a = l - r_1$ is the distance between the hip and the center of mass of swing-leg when the leg is straightened. In addition, we make the foot radius larger to reduce energy dissipation on collisions at the ground [4]. A knee-joint torque is designed to make the distance between the hip and the center of mass, L_c , to track the reference trajectory (10). The reference trajectory of $\theta_2 - \theta_3$ is calculated from

$$L_c = L_{cd}, \quad (11)$$

and the trajectory is given by

$$h(t) = (\theta_2 - \theta_3)_d = -\arccos(F_4 L_{cd}^2 - F_3), \quad (12)$$

where

$$F_3 = \frac{F_1}{F_2}, \quad (13)$$

and

$$F_4 = \frac{(m_2 + m_3)^2}{F_2}. \quad (14)$$

If we define $\mathbf{x} = [\theta_1 \quad \theta_2 \quad \theta_2 - \theta_3 - h]^T$, then $\boldsymbol{\theta}$ is rewritten by

$$\boldsymbol{\theta} = \begin{bmatrix} 1 & 0 & 0 \\ 0 & 1 & 0 \\ 0 & 1 & -1 \end{bmatrix} \mathbf{x} + \begin{bmatrix} 0 \\ 0 \\ -h \end{bmatrix} =: \mathbf{Q}\mathbf{x} + \mathbf{N}, \quad (15)$$

$\dot{\boldsymbol{\theta}}$ and $\ddot{\boldsymbol{\theta}}$ then yield

$$\dot{\boldsymbol{\theta}} = \mathbf{Q}\dot{\mathbf{x}} + \dot{\mathbf{N}}, \quad (16)$$

$$\ddot{\boldsymbol{\theta}} = \mathbf{Q}\ddot{\mathbf{x}} + \ddot{\mathbf{N}}. \quad (17)$$

The dynamic equation (1) is redefined as

$$\mathbf{M}\mathbf{Q}\ddot{\mathbf{x}} + \mathbf{M}\ddot{\mathbf{N}} + \mathbf{C}\mathbf{Q}\dot{\mathbf{x}} + \mathbf{C}\dot{\mathbf{N}} + \mathbf{g} = \mathbf{S}u_K. \quad (18)$$

Since proposal robot has a knee actuation only (Fig. 1), the control input vector is given by

$$\mathbf{S} = \begin{bmatrix} 0 \\ -1 \\ 1 \end{bmatrix}. \quad (19)$$

TABLE I
PHYSICAL PARAMETERS OF THE KNEED BIPED ROBOT.

r_1	0.350	m	R	0.65	m
r_2	0.25	m	$m_1 (= m_2 + m_3)$	5.0	kg
r_3	0.25	m	m_2	1.0	kg
a_2	0.50	m	m_3	4.0	kg
a_3	0.50	m	m_H	5.5	kg
$l (= a_2 + a_3)$	1.00	m			

Let define K as

$$K = [0 \quad 0 \quad 1] \mathbf{Q}^{-1} [\mathbf{M}^{-1}\mathbf{S}], \quad (20)$$

and the knee torque u_K as

$$u_K = K^{-1}(v + Z), \quad (21)$$

where v is a input expressed soon, and Z is defined as

$$Z = [0 \quad 0 \quad 1] \mathbf{Q}^{-1} \mathbf{M}^{-1} (\mathbf{M}\mathbf{N} + \mathbf{C}\mathbf{Q}\dot{\mathbf{x}} + \mathbf{C}\dot{\mathbf{N}} + \mathbf{g}). \quad (22)$$

Then, dynamic equation (18) is rewritten by partial feedback linearization as

$$\ddot{y} = v, \quad (23)$$

where $y = \theta_2 - \theta_3 - h$. The input v is designed by PD control to converge to the reference trajectory.

C. Simulation results

Table I shows the parameters of the biped robot of Fig. 1 used in our numerical simulation. In our method, the knee torque can not be calculated at the initial state which is the first part of the 1st phase shortly after the 3rd phase. This is because derivative of reference trajectory, $\dot{h}(t)$, is given by

$$\dot{h}(t) = \frac{2F_4 L_{cd} \dot{L}_{cd}}{\sqrt{1 - (F_4 L_{cd}^2 - F_3)^2}} \quad (24)$$

and $(F_4 L_{cd}^2 - F_3) \approx 1$ holds at the initial state. Instead, the knee torque, u_K , is given by Eq. (12) only when $(F_4 L_{cd}^2 - F_3) \leq 0.999$, and is set to zero when $(F_4 L_{cd}^2 - F_3) > 0.999$.

Simulation results of parametric excitation walking by knee-joint's actuation in the case when $A_m = 0.078$ and $T_{set} = 1.2$ are shown in Fig. 9 which illustrates a few steps after sufficient time. In this approach, a sustainable gait can be generated without a hip torque. Fig. 9 (a) shows angles, (b) shows angular velocities, (c) shows the total mechanical energy, (d) shows knee torque, (e) shows foot clearance and (f) shows distance between the hip joint and the center of mass of the swing-leg. From Figs. 9 (c) and (f), it is observed that the total mechanical energy is restored when a knee of biped robot is bended and that the total energy is reduced when a knee is stretched. The difference between the increase energy and the decrease energy is the quantity of total energy restoration. From Fig. 9 (c), energy dissipation of the collision at the knee is almost negligible. In Figs. 9 (c) and (d), total mechanical energy is constant when the knee torque is zero. We expected to avoid digging the ground in our approach, however, it is observed from Fig. 9 (e) that this biped robot unfortunately digs the ground because this robot has big soles shown in Fig. 10.

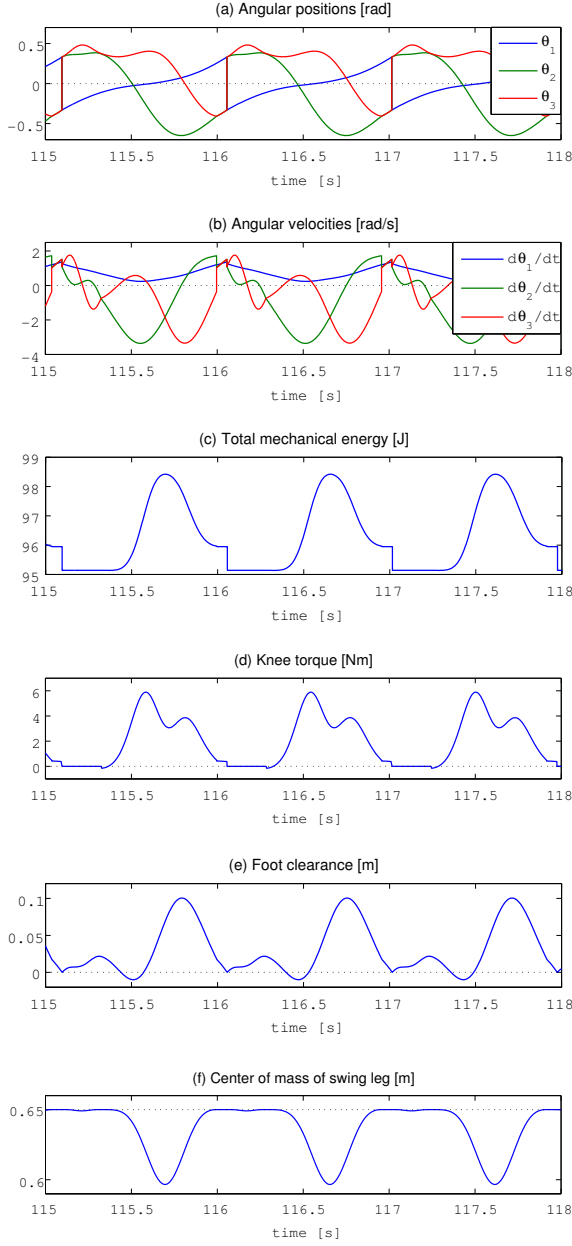


Fig. 9. Simulation results of revolutionary parametrically excited walking.

IV. EFFECT OF PARAMETERS

In this section, we discuss the effect of desired amplitude of vibration, A_m , and the desired settling-time, T_{set} with foot radius, R , 0.65, 0.675 and 0.70. We evaluate walking period, walking speed and specific resistance. Specific resistance defined by

$$\mu = \frac{\int_{0^+}^{T^-} |u_K(\dot{\theta}_2 - \dot{\theta}_3)| dt / T}{M_g g \bar{V}} \quad (25)$$

represents energy efficiency, and the smaller this value is the more efficient. 0^+ and T^- in Eq. 25 represent the time after collision at the ground and the time before collision at the

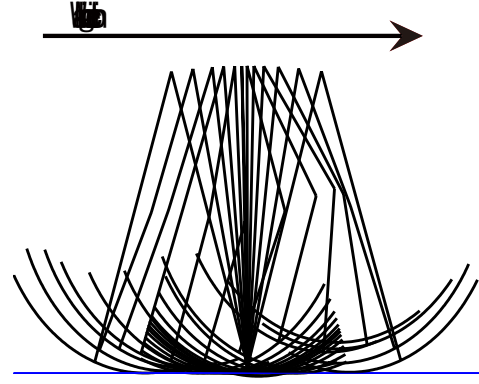


Fig. 10. Stick diagram of revolutionary parametrically excited walking.

ground, respectively, M_g is the total mass of a biped robot and \bar{V} is average speed.

Simulation results are shown in Figs. 11 and 12. In the Figs. the blue lines with square points are the results of $R = 0.65$, the green lines with circle points are the results of $R = 0.675$, and the red lines with triangle points are the results of $R = 0.7$. Fig. 11 shows the effect of desired amplitude of vibration and (a) shows walking period, (b) shows walking speed and (c) shows specific resistance at $T_{set} = 1.15$. It is observed from Fig. 11 that walking period, walking speed and specific resistance increase when desired amplitude of vibration increases.

Fig. 12 shows the effect of desired settling-time and (a) shows walking period, (b) shows walking speed and (c) shows specific resistance at $A_m = 0.0975$. Fig. 12 shows that walking period and walking speed increase and specific resistance decreases when desired amplitude of vibration increases. In Figs. 11 and 12, walking period and walking speed increase, and specific resistance decreases when the foot radius is larger.

Figs. 11 (a) and 12 (a) show that the settling-time condition is not satisfied, that is $T < T_{set}$. This is because $u_K = 0$ near the initial state lead to deviation from the reference trajectory, then overshoot occurs by PD control, and hence a collision at the knee occurs before T_{set} .

V. CONCLUDING REMARKS

In this paper, we have presented the sustainable gait generation method based on parametric excitation principle without the hip torque for the rotary actuation system. The reference trajectory is given by the distance between the hip joint and the mass of the swing-leg. But the proposed method has the problem that h in Eq. (12) can not be calculated near the initial state. Therefore, the knee torque is set to zero at that time. In addition, because a power of sin is 11, duration of $F_4 L_{cd}^2 - F_3 \approx 1$ is long and hence, the deviation from reference trajectory occurs. To resolve this problem, we consider another reference trajectory which is given to

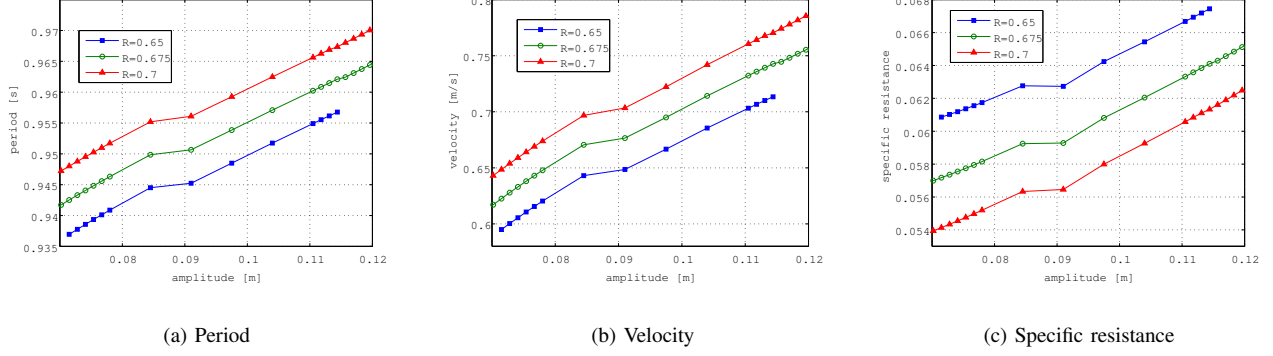


Fig. 11. Effect of the desired amplitude of vibration A_m .

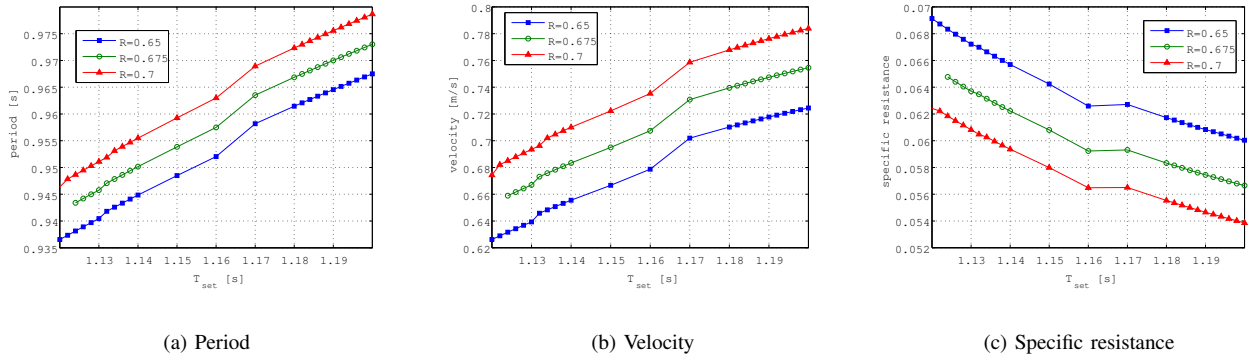


Fig. 12. Effect of the desired settling-time T_{set} .

relative angle of the knee by

$$(\theta_2 - \theta_3)_d = \begin{cases} \theta_0 \sin^n \left(\frac{\pi}{T_{set}} t \right) & (t \leq T_{set}) \\ 0 & (t > T_{set}). \end{cases} \quad (26)$$

We now simulate according to Eq. (26).

There is another problem that this biped robot digs the ground because it has big soles to reduce energy dissipation. For this problem, we will use the hip torque as well as the knee torque to restore more mechanical energy and then to make the sole size of a biped robot smaller.

In our model, the specific resistance is smaller as the desired settling-time is larger. On the other hand the specific resistance is larger as the desired amplitude of vibration is larger, even though walking speed is also larger. This phenomenon is of much interest and to resolve it is a subject of one of future research.

VI. ACKNOWLEDGMENTS

This research is partly supported by the Japanese Center of Excellence program 'Micro- and Nano-Mechanics for Information-Based Society' (2003-2007).

REFERENCES

- [1] F. Asano and Z.W. Luo, "On energy-efficient and high-speed dynamic biped locomotion with semicircular feet," *IEEE/RSJ Int. Conf. on Intelligent Robotics and Systems*, 2006.
- [2] F. Asano, Z.W. Luo and S. Hyon, "Parametric excitation mechanisms for dynamic bipedal walking," *IEEE Int. Conf. on Robotics and Automation*, 2005.
- [3] F. Asano, M. Yamakita and K. Furuta, "Virtual passive dynamic walking and energy-based control Laws," *IEEE/RSJ Int. Conf. on Intelligent Robotics and Systems*, 2000.
- [4] F. Asano and Z.W. Luo, "The effect of semicircular feet on energy dissipation by heel-strike in dynamic bipedal locomotion," *IEEE Int. Conf. on Robotics and Automation*, 2007.
- [5] A. Goswami, B. Espiau and A. Keramane, "Limit cycles in a passive compass gait biped and passivity-mimicking control laws," *J. of Autonomous Robots*, vol. 4, no. 3, 1997, pp 273-286.
- [6] Y. Harata, Z.W. Luo, F. Asano, K. Taji and Y. Uno, "Dynamic control for a biped walking robot based on virtual constraints (in Japanese)," *the 49th Japan Joint Automatic Control Conf. (JJACC)*, 2006.
- [7] E.K. Lavrovskii and A.M. Formalskii, "Optimal control of the pumping and damping of swing," *J. of Applied Mathematics and Mechanics*, vol. 57, no. 2, 1993, pp 311-320.
- [8] T. McGeer, "Passive dynamic walking," *Int. J. of Robotics Research*, vol. 9, no. 2, 1990, pp 62-82.
- [9] A. Vukobratović and D. Juričić, "Contribution to the synthesis of biped gait," *IEEE Trans. on Bio-Medical Engineering*, vol. 16, no. 1, 1969, pp 1-6.